

Photoacoustic Imaging of the Bladder

A Pilot Study

Aya Kamaya, MD, Srikant Vaithilingam, MS, Benjamin I. Chung, MD, Omer Oralkan, PhD,
Butrus T. Khuri-Yakub, PhD

Photoacoustic imaging is a promising new technology that combines tissue optical characteristics with ultrasound transmission and can potentially visualize tumor depth in bladder cancer. We imaged simulated tumors in 5 fresh porcine bladders with conventional pulse-echo sonography and photoacoustic imaging. Isoechoic biomaterials of different optical qualities were used. In all 5 of the bladder specimens, photoacoustic imaging showed injected biomaterials, containing varying degrees of pigment, better than control pulse-echo sonography. Photoacoustic imaging may be complementary to diagnostic information obtained by cystoscopy and urine cytologic analysis and could potentially obviate the need for biopsy in some tumors before definitive treatment.

Key Words—bladder cancer; bladder tumor depth; bladder tumor staging; noninvasive bladder cancer staging; optoacoustic imaging; photoacoustic imaging

Received April 25, 2012, from the Department of Radiology, Stanford University Medical Center, Stanford, California USA (A.K., B.I.C.); Stanford University, Stanford, California USA (S.V.); Department of Electrical and Computer Engineering, North Carolina State University, Raleigh, North Carolina USA (O.O.); and E. L. Ginzton Laboratory, Center for Nanoscale Science and Engineering, Stanford University, Stanford, California USA (B.T.K.-Y.). Revision requested June 12, 2012. Revised manuscript accepted for publication November 16, 2012.

We thank Jeslyn A. Rumbold for assistance with manuscript preparation. This work was funded by a Society of Uroradiology 2011 research grant.

Address correspondence to Aya Kamaya, MD, Department of Radiology, Stanford University Medical Center, 300 Pasteur Dr, Stanford, CA 94305 USA.

E-mail: kamaya@stanford.edu

Abbreviations

ICG, indocyanine green

doi: 10.7863/ultra.32.7.1245

Bladder cancer is the second most common cancer of the genitourinary tract, accounting for 7% of all new cancer cases in men and 2% of new cancer cases in women.¹ Patients typically present with hematuria, which may be gross or microscopic, and can have symptoms of urinary frequency, urgency, or dysuria.¹ Pathologic stage T1 tumors are treated with complete transurethral resection and often with intravesical immunotherapy or chemotherapy, whereas pathologic stage T2 tumors are generally treated with radical cystectomy. Currently, clinical staging is limited by the lack of accuracy in available preoperative imaging modalities, such as transabdominal sonography, computed tomography, and magnetic resonance imaging, with overall staging accuracy ranging from 40% to 85% for computed tomography and 50% to 90% for magnetic resonance imaging.^{2,3} The biggest limitation of imaging is determining the presence of muscularis propria invasion.⁴ Because transurethral resection of pathologic T1 bladder tumors may result in considerable understaging,⁵ second-look transurethral resection procedures are routinely performed to eliminate this possibility.⁶ However, deep biopsy of bladder tumors may lead to bladder perforation, requiring surgical repair and increasing the risk of tumor seeding. If an imaging modality existed that could lessen the understaging errors inherent to transurethral resection, the surgeon could proceed directly to radical cystectomy in patients with pathologic T2 tumors. Therefore, there is a need for accurate staging of bladder cancer to assess tumor depth to help guide appropriate treatment and obviate the need for invasive procedures.

Photoacoustic imaging is a hybrid technology combining tissue optical characteristics with ultrasound transmission. Tissue is illuminated with short laser pulses and, depending on the optical characteristics, absorbs the light in varying degrees, causing the tissue to heat imperceptibly and expand, which in turn generates acoustic pressure waves due to the thermoelastic effect, which can be detected and imaged. The varying amount of absorbed light provides contrast information, which is transmitted as an ultrasound signal. Because ultrasound waves are less susceptible to scatter than light waves, photoacoustic imaging is able to combine the contrast information of optical imaging with the spatial resolution of acoustic imaging.⁷ Photoacoustic imaging also has the ability to differentiate structures based on color, which could potentially be effective in diagnosing bladder cancer because of their intrinsic hypervascularity.

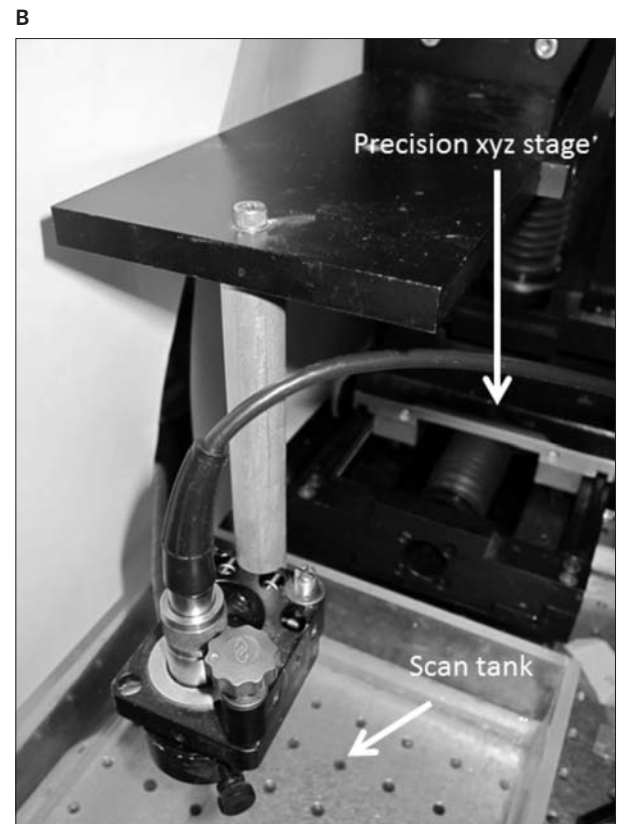
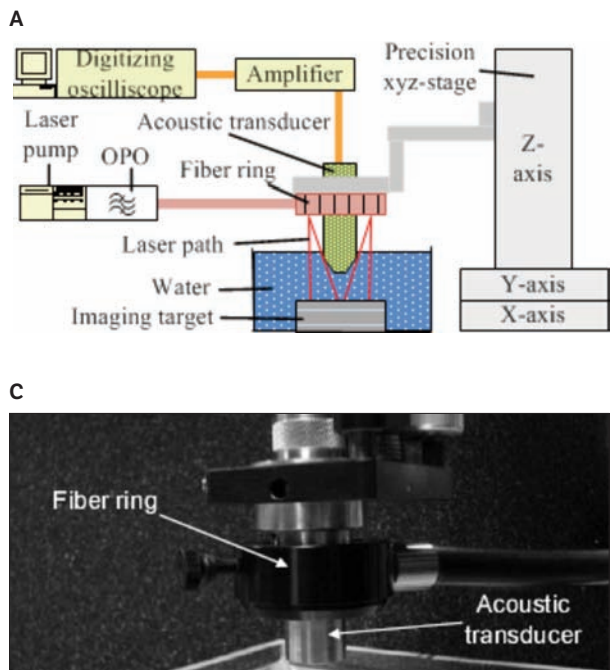
Photoacoustic imaging has the potential to be highly effective in the diagnosis and staging of bladder tumors with transurethral imaging because of the relatively thin nature of the underlying bladder wall and the need for high spatial resolution in tumor staging to assess tumor invasion depth. We report a pilot study in which cadaver porcine bladders were imaged with conventional pulse-echo

sonography and photoacoustic imaging with different biomaterials injected within the bladder wall to determine the efficacy in staging these tumors in real time.

Materials and Methods

In our ultrasound laboratory, we developed a coaxial scanning acoustic/photoacoustic microscope (Figure 1). In our microscopy system, the laser source is an optical parametric oscillator pumped by a Q-switched neodymium–yttrium aluminum garnet laser (Surelite SLIII-10; Continuum, Santa Clara, CA). Laser pulses with a pulse width of 5 nanoseconds and a repetition rate of 10 Hz are coupled into an optical fiber. The distal end of the fiber terminates in a fiber-optic ring coaxial with the ultrasound transducer. The transducer is mounted through the central hole in the fiber-optic ring, resulting in laser illumination coaxial with the ultrasound detection. The transducer and fiber-optic ring are mounted together on a precision xyz stage (Aerotech, Inc, Pittsburgh, PA) with a minimum step size of 1 μm (Figure 1), and a personal computer controls the movement of the xyz stage. In the photoacoustic mode, the sample is irradiated with laser pulses that induce acoustic

Figure 1. Photoacoustic imaging setup. **A**, Labeled schematic of the setup. OPO indicates optical parametric oscillator. **B**, Setup showing the precision xyz stage and scan tank. **C**, Close-up view of the transducer holder and fiber ring.



Author: The unit cc is changed to mL, per American Medical Association style. In Table 1, please verify manufacturer of Matrigel as added.

waves, which are detected by the ultrasound transducer. The fiber-optic ring focuses the laser beam to a diameter of approximately 1 cm at the point of imaging. The average energy density of the laser is approximately 9 mJ/cm^2 at the target site. The sample is raster scanned to obtain a complete 3-dimensional image. A focused ultrasound transducer with a center frequency of 25 MHz, a diameter of 0.25 in, and a focal length of 1 in (V324; Panametrics, Waltham, MA) is used in the system. The optical parametric oscillator is set to a wavelength of 780 nm. The photoacoustic signals received by the ultrasound transducer are amplified by an amplifier (PR5058; Panametrics) and recorded by a digitizing oscilloscope (Infiniium DSO8104A; Agilent Technologies, Palo Alto, CA). In the pulse-echo mode, the laser is turned off, and a high-voltage, spike-type electronic pulser (PR5058; Panametrics) is used to excite the ultrasound transducer.

The photoacoustic and pulse-echo images are reconstructed as follows: The A-scan from each (x, y) position of the transducer is bandpass filtered and envelope detected before being combined to reconstruct a 3-dimensional intensity image of the target; the image is then logarithmically compressed according to the dynamic range desired. In the acoustic images, the intensity represents the acoustic reflectivity of the target, whereas in the photoacoustic images, the intensity represents the optical absorption coefficient of the target. The photoacoustic and

pulse-echo images are coregistered at the end. Photoacoustic images are averaged 8 times; thus, it takes approximately 10 minutes to complete a photoacoustic line scan.⁸

Five porcine bladders were injected with 5 separate biomaterials of varying optical qualities (Table 1) selected for their relatively isoechoic appearance on grayscale imaging. These biomaterials were selected because of their ability to closely approximate the imaging qualities of transitional cell carcinoma of the bladder. Approximately 0.5 mL of each biomaterial was injected submucosally. The bladders were then placed in a 10% agar solution until the agar solidified and then placed in a water bath to allow for optimal sonographic and photoacoustic imaging. The bladders were imaged with both pulse-echo sonography at 10 to 25 MHz and photoacoustic imaging with a laser wavelength of 780 nm. Indocyanine green (ICG) concentrations of 64 and 128 μM were chosen because these wavelengths correspond to relative peak absorptions of ICG at 780 nm. Image pixel analysis of each bladder was performed to quantify the degree of visualization on photoacoustic imaging compared to conventional grayscale imaging using AMIDE (A Medical Image Data Examiner) software (<https://cpacs.stanfordmed.org/ami/html>), an open-source tool used to analyze medical imaging data sets.⁹

Results

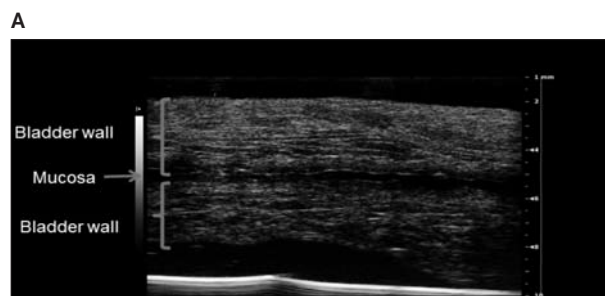
Five porcine bladders were simultaneously imaged with photoacoustic imaging and pulse-echo sonography. Image overlays were obtained, superimposing the photoacoustic images onto the pulse-echo images. In addition to the combined photoacoustic and pulse-echo imaging, high-resolution pulse-echo sonography was performed at 40 MHz in one bladder specimen on a commercially available Vevo 2100 animal ultrasound machine (VisualSonics, Toronto, Ontario, Canada; Figure 2A), which showed excellent

Table 1. Biomaterials and Corresponding Optical Materials Used for Imaging Experiments

Specimen	Biomaterial	Optical Material
1	Carrot puree	Carrot puree
2	Gelatin + cellulose	ICG
3	Matrigel ^a	ICG
4	Gelatin + cellulose	ICG
5	Gelatin + cellulose vs Matrigel	ICG

^aBD Biosciences (Franklin Lakes, NJ).

Figure 2. **A**, High-resolution sonogram of a bladder showing excellent visualization of bladder wall layers and mucosa. **B**, Injected biomaterials are mildly visible on a high-resolution sonogram of the bladder and can be seen in the subserosal area within muscular layers. Fluid is seen in the lumen of the bladder.



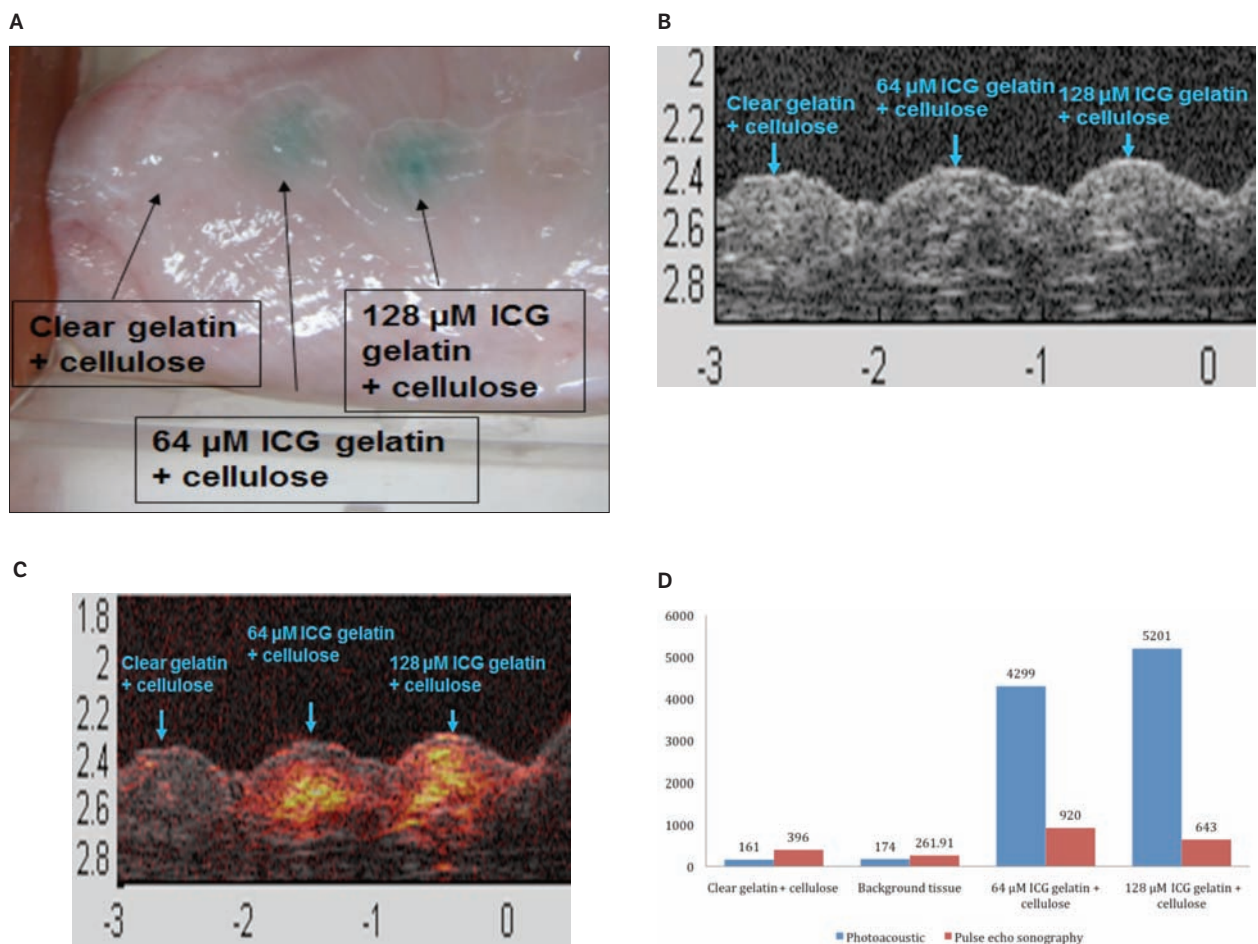
visualization of the bladder wall muscle layers and the injected biomaterial in the bladder wall (Figure 2B).

Pulse-echo sonography at 25 MHz and simultaneous photoacoustic imaging at 780 nm with a 25-MHz transducer was performed on bladder specimens injected with biomaterials. In these specimens, the injected materials were less visible in the bladder wall on pulse-echo sonography compared to photoacoustic imaging (Figure 3, A and B). The photoacoustic images showed greatly improved contrast of the biomaterials compared to the background bladder (Figure 3C). In all 5 bladders, the injected areas of interest were well visualized on photoacoustic imaging

compared to conventional sonography alone. There also was a stronger photoacoustic signal with higher micromolar concentrations of injected ICG. Conversely, colorless controls and the background bladder did not generate a strong photoacoustic signal.

Photoacoustic imaging of bladders injected with a combination of ICG, gelatin, and cellulose showed a 17-fold signal increase at the ICG concentration of 64 μM and a 19-fold increase at 128 μM , whereas on pulse-echo sonography, the signal did not change substantially from that of the background tissue, with only a 2.3-fold increase at 64 μM and a 1.6-fold increase at 128 μM (Figure 3D).

Figure 3. **A**, Bladder injected with clear gelatin + cellulose and gelatin + cellulose mixed with ICG at concentrations of 64 and 128 μM . The bladder has been everted to show the mucosa. **B**, Pulse-echo sonogram of the bladder with injected material. Optical differences are not appreciated on conventional sonography. **C**, Photoacoustic image overlaid on the sonogram clearly showing areas with ICG compared to colorless controls. The area injected with clear gelatin + cellulose shows little if any photoacoustic signal, whereas the area injected with 64- μM ICG shows a substantial photoacoustic signal, and the area injected with 128- μM ICG shows the greatest photoacoustic signal. **D**, Mean pixel counts for photoacoustic imaging and pulse-echo sonography of the same specimen. Photoacoustic imaging shows a clear signal with gelatin + cellulose mixed with 64- and 128- μM ICG to a much better extent than pulse-echo sonography.



Discussion

Although most bladder tumors are well visualized optically with conventional cystoscopy, the depth of invasion cannot be assessed without biopsy, which can lead to understaging errors and surgical complications. In our pilot study, we were able to visualize the location and depth of the biomaterials in the bladder wall with photoacoustic imaging and pulse-echo sonography. The photoacoustic images showed excellent contrast of the materials from the background bladder, and pulse-echo sonography showed anatomic detail with excellent visualization of bladder layers. The combination of these imaging modalities provides complementary and useful information not currently clinically available.

To our knowledge, no other investigators have examined the feasibility of using photoacoustic imaging for evaluation of bladder cancer. Although a recent study by Kim et al¹⁰ showed that photoacoustic imaging could visualize the lumen of a rat bladder filled with methylene blue, they did not attempt to visualize the bladder wall itself, nor did they evaluate whether any features of bladder irregularity could be discerned. In addition, theirs was a pilot study in which only a single rat was imaged.

Other investigators have looked at other methods to noninvasively image urothelial tumors. Wang et al^{11,12} used endoscopic optical coherence tomography for evaluation of bladder and ureteral walls to visualize superficial tumors with promising initial results. They acknowledged, however, that this modality can only visualize 1 to 2 mm in depth and proposed that their technology be primarily used for identification of invisible but suspected tumors in the setting of positive bladder washings for very early tumors or carcinoma in situ.¹¹

Our application of photoacoustic imaging is different from that of other investigators in that we propose that this imaging modality be used for clearly visible bladder tumors in which tumor staging is important for treatment. More specifically, photoacoustic imaging should be used for delineation of tumor extension into the muscularis propria and potentially the perivesical fat. Clear and accurate diagnosis of pathologic stage T2 disease would allow one to proceed directly to radical cystectomy without the delay of awaiting final pathologic results. Pathologic stage T3 disease cannot currently be diagnosed with standard biopsy techniques, and accurate diagnosis of stage T3 disease would allow for consideration of neoadjuvant chemotherapy. Although a major limitation of photoacoustic imaging is depth penetration, in our experience, photoacoustic imaging can be easily performed up to depths of 4 to 5 cm, well beyond the levels necessary for bladder imaging.¹³

There are some potential limitations of photoacoustic imaging in bladder cancer. Although most bladder tumors are hyperemic because of increased angiogenesis, carcinomas in situ and nonhyperemic tumors may potentially be less visible on photoacoustic imaging. Differences in optical absorption of a tumor versus the background bladder determine visualization with this imaging modality; therefore, nonhyperemic tumors may be understaged. We used ICG, a molecule with optical properties well characterized and approved by the US Food and Drug Administration for human use, as a substitute for a hyperemic bladder mass. We could overcome this potential limitation by using ICG in tumor imaging, in which ICG could be tagged to another intravenous agent or potentially used in its simple form for tumor evaluation with photoacoustic imaging, which could improve visualization of bladder tumors. Other contrast agents for photoacoustic imaging, such as gold nanoparticles, have been studied by other investigators¹⁴ and may be used for bladder tumor imaging to improve imaging accuracy.

Because this study was a pilot and feasibility study performed on fresh cadaver porcine bladders injected with biomaterials to simulate bladder cancer, future studies will need to be performed on humans with true bladder tumors at varying degrees of invasion to determine the true clinical efficacy of photoacoustic imaging. Currently, no animal model of bladder cancer is available for in vivo imaging. Other investigators have used bladder irritants to simulate hyperemia seen in bladder cancer.¹¹ However, these irritants are surrogates for true bladder cancer and carry inherent limitations.

In our study, we performed imaging with a coaxial scanning acoustic/photoacoustic microscope. However, we envision future bladder imaging using a transurethral ultrasound catheter, which can obtain 3-dimensional images of the bladder wall and surrounding tissue with high resolution ($\approx 150 \mu\text{m}$). The proposed imaging device is a ring-shaped transducer array with an inner lumen available for introducing an optical fiber through which short laser pulses illuminate tissue for photoacoustic imaging. This catheter may provide both anatomic sonograms and photoacoustic information to help delineate malignant tumors. The same inner lumen can also be used as a delivery port to introduce a biopsy tool or single high-frequency focused transducer to apply high-intensity focused ultrasound to the tumor for treatment. A 12F prototype catheter based on capacitive micromachined ultrasound transducer technology has already been developed in our laboratory and used for in vivo intracardiac sonography in a porcine model to guide electrophysiologic interventions.¹⁵ This catheter can easily be used for future transurethral bladder imaging.

Author: Please verify page numbers as added for reference 1.

In conclusion, current imaging modalities do not accurately stage transitional cell carcinoma of the bladder and cannot assess tumor depth without invasive biopsy procedures. Photoacoustic imaging in combination with high-resolution pulse-echo sonography has the potential to stage bladder tumor extension before excision or even preclude the need for standard biopsy techniques for diagnosis, which could guide treatment and prevent unnecessary procedures before definitive treatment.

References

- Konety BR, Carroll PR. Urothelial carcinoma: cancers of the bladder, ureter, & renal pelvis. In: Tanagho EA, McAninch JW (eds). *Smith's General Urology*. 17th ed. New York, NY: McGraw-Hill; 2007:308–327.
- Fisher MR, Hricak H, Tanagho EA. Urinary bladder MR imaging, part II: neoplasm. *Radiology* 1985; 157:471–477.
- Wood DP Jr, Lorig R, Pontes JE, Montie JE. The role of magnetic resonance imaging in the staging of bladder carcinoma. *J Urol* 1988; 140:741–744.
- Barentsz JO, Jager GJ, Witjes JA, Ruijs JH. Primary staging of urinary bladder carcinoma: the role of MRI and a comparison with CT. *Eur Radiol* 1996; 6:129–133.
- Divrik RT, Sahin AF, Yildirim U, Altok M, Zorlu F. Impact of routine second transurethral resection on the long-term outcome of patients with newly diagnosed pT1 urothelial carcinoma with respect to recurrence, progression rate, and disease-specific survival: a prospective randomised clinical trial. *Eur Urol* 2010; 58:185–190.
- Dalbagni G. Bladder cancer: restaging TUR reduces recurrence and progression risk. *Nat Rev Urol* 2010; 7:649–650.
- Wang LV. Ultrasound-mediated biophotonic imaging: a review of acousto-optical tomography and photo-acoustic tomography. *Dis Markers* 2003; 19:123–138.
- Vaithilingam S, Ma TJ, Furukawa Y, et al. A co-axial scanning acoustic and photoacoustic microscope. *Proc IEEE Ultrason Symp* 2007; 2007:2413–2416.
- Loening AM, Gambhir SS. AMIDE: a free software tool for multimodality medical image analysis. *Mol Imaging* 2003; 2:131–137.
- Kim C, Jeon M, Wang LV. Nonionizing photoacoustic cystography in vivo. *Opt Lett* 2011; 36:3599–3601.
- Wang Z, Lee CS, Waltzer WC, Liu J, Xie H, Yuan Z, et al. In vivo bladder imaging with microelectromechanical-systems-based endoscopic spectral domain optical coherence tomography. *J Biomed Opt* 2007; 12:034009.
- Wang H, Kang W, Zhu H, MacLennan G, Rollins AM. Three-dimensional imaging of ureter with endoscopic optical coherence tomography. *Urology* 2011; 77:1254–1258.
- Ma TJ, Kothapalli SR, Vaithilingam S, et al. 3-D deep penetration photoacoustic imaging with a 2-D CMUT array. *Proc IEEE Ultrason Symp* 2010; 2010:375–377.
- De La Zerda A, Zavaleta C, Keren S, et al. Carbon nanotubes as photoacoustic molecular imaging agents in living mice. *Nat Nanotechnol* 2008; 3:557–562.
- Nikoozadeh A, Oralkan Ö, Gencel M, et al. Forward-looking intracardiac imaging catheters using fully integrated CMUT arrays. *Proc IEEE Ultrason Symp* 2010; 2010:770–773.